Volume 27
Number 8
28 February 2025
Pages 4009–4498

PCCP

Physical Chemistry Chemical Physics

rsc.li/pccp

25 YEARS ANNIVERSARY

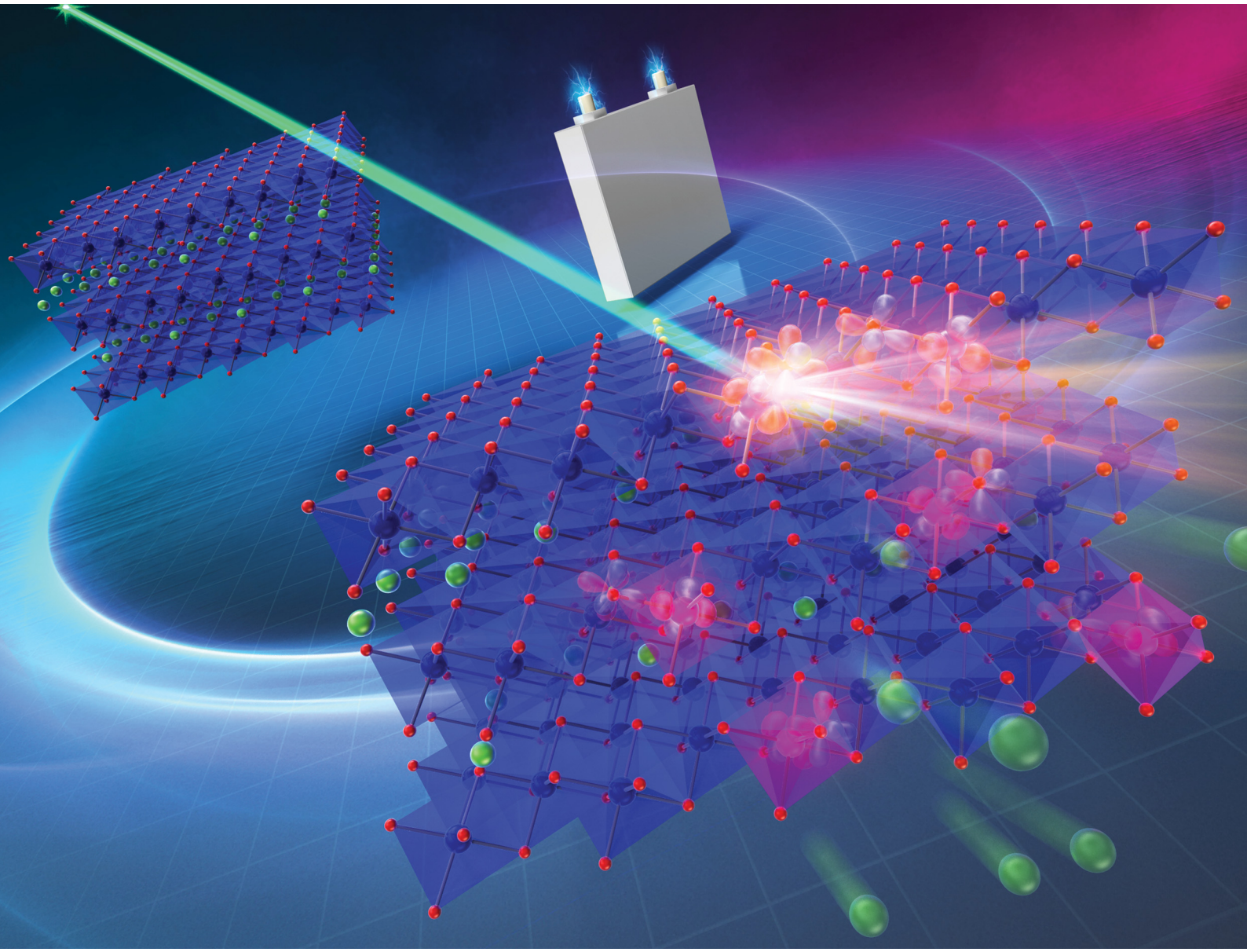

ISSN 1463-9076

ROYAL SOCIETY OF CHEMISTRY

PAPER

Daisuke Asakura *et al.*

Elucidation of the Co^{4+} state with strong charge-transfer effects in charged $LiCoO_2$ by resonant soft X-ray emission spectroscopy at the Co L_3 edge

PCCP Owner Societies

PCCP

PAPER

View Article Online
View Journal | View Issue

Cite this: *Phys. Chem. Chem. Phys.*, 2025, **27**, 4092

Elucidation of the Co^{4+} state with strong charge-transfer effects in charged $LiCoO_2$ by resonant soft X-ray emission spectroscopy at the Co L_3 edge

Daisuke Asakura, *[abc] Takaaki Sudayama,[a] Yusuke Nanba, †[a] Eiji Hosono, [abc] Hisao Kiuchi,[de] Kosuke Yamazoe,[de] Jun Miyawaki,‡[de] Yoshihisa Harada, [cde] Atsuo Yamada, [fg] Ru-Pan Wang §[h] and Frank M. F. de Groot [h]

Received 30th September 2024,
Accepted 7th December 2024

DOI: 10.1039/d4cp03759f

rsc.li/pccp

To understand the electronic-structure change of $LiCoO_2$, a widely used cathode material in Li-ion batteries, during charge–discharge, we performed *ex situ* soft X-ray absorption spectroscopy (XAS) and resonant soft X-ray emission spectroscopy (RXES) of the Co L_3 edge in combination with charge-transfer multiplet calculations. The RXES profile significantly changed for the charged state at 4.2 V *vs.* Li/Li^+, corresponding to the oxidation reaction from a Co^{3+} low-spin state for the initial state, while the XAS profile exhibited small changes. For the 4.2-V charged state, we confirmed that approximately half of the initial Co^{3+} ions were oxidized to Co^{4+} ions. The multiplet calculation of the RXES results revealed that the Co^{4+} state has a negative charge-transfer energy and the $d^6\underline{L}$ state ($\underline{L}$ is a ligand hole) is the most stable. Therefore, the O 2p hole created by the strong charge-transfer effect plays a major role in the redox reaction of $LiCoO_2$.

1. Introduction

In the past few decades, Li-ion batteries (LIBs) have been extensively developed for various applications. To apply LIBs to electric vehicles and large-scale energy-storage systems, their energy density and safety need to be improved. Increasing the charge–discharge capacity of the cathodes of LIBs is particularly important for increasing the energy density. The charge–discharge capacity is directly connected with the redox reaction. In the case of $LiCoO_2$, which is a typical cathode material, the formal valence of Co changes according to the equation $LiCo^{3+}O_2 \Leftrightarrow 0.5Li^+ + 0.5e^- + Li_{0.5}Co^{4+}{}_{0.5}Co^{3+}{}_{0.5}O_2$ with charge (Li extraction)/discharge (Li insertion) within a cutoff voltage range of 3.0–4.2 V (*vs.* Li/Li^+), where the capacity is approximately 150 mA h g^{-1}.[1,2] To confirm the Co^{3+}/Co^{4+} redox reaction, many groups have investigated the electronic structure of $LiCoO_2$ by various methods.[1–9] X-ray absorption spectroscopy (XAS) is one of the most powerful tools to analyze the electronic structure of cathode materials. In the case of 3d transition-metal (TM) oxides (TMOs) involving $LiCoO_2$, TM K-edge (mainly the 1s → 4p transition) and $L_{2,3}$-edge XAS ($2p_{1/2,3/2}$ → 3d transition) have been extensively performed. For example, the Co^{3+} low-spin state has been confirmed to be the initial state of $LiCoO_2$ by Co K-edge and $L_{2,3}$-edge XAS.[8–16] For the charge process of $LiCoO_2$, Co K-edge XAS studies have shown that the main peak shifts to the high-energy side, and Co $L_{2,3}$-edge XAS studies have revealed that the XAS line shape changes, which suggest the oxidation reaction from the Co^{3+} state to the Co^{4+} state.[15,16]

In this study, we focus on the Co^{4+} state in the charge process because the electronic configuration and Co 3d–O 2p

[a] *Research Institute for Energy Conservation, National Institute of Advanced Industrial Science and Technology (AIST), Tsukuba, Ibaraki 305-8585, Japan. E-mail: daisuke-asakura@aist.go.jp*
[b] *Global Zero Emission Research Center, National Institute of Advanced Industrial Science and Technology (AIST), Tsukuba, Ibaraki 305-8589, Japan*
[c] *AIST-UTokyo Advanced Operando Measurement Technology Open Innovation Laboratory (Operando OIL), Kashiwa, Chiba 277-8565, Japan*
[d] *Institute for Solid State Physics (ISSP), The University of Tokyo, Kashiwa, Chiba 277-8581, Japan*
[e] *Synchrotron Radiation Research Organization (SRRO), The University of Tokyo, Sendai, Miyagi 980-8572, Japan*
[f] *Department of Chemical System Engineering, The University of Tokyo, Bunkyo-ku, Tokyo 113-8656, Japan*
[g] *Sungkyunkwan University Institute of Energy Science & Technology (SIEST), Sungkyunkwan University, Suwon 16419, South Korea*
[h] *Debye Institute for Nanomaterials Science, Utrecht University, 3584 GG Utrecht, The Netherlands*
† Present address: Research Initiative for Supra-Materials, Shinshu University, Nagano, Nagano 380-8553, Japan.
‡ Present address: NanoTerasu Center, National Institutes for Quantum Science and Technology, Sendai, Miyagi 980-8579, Japan.
§ Present address: Deutsches Elektronen Synchrotron DESY, Hamburg 22607, Germany.

orbital hybridization of the Co–O bond have been unclear. Resonant soft X-ray emission spectroscopy (RXES) combined with theoretical charge-transfer (CT) multiplet calculations is a promising method to investigate the Co 3d electronic structure. RXES is the secondary process after XAS, reflecting the element and orbital-selective occupied (valence) state.[17–19] Recently, RXES has attracted considerable interest for studying electrode materials,[20–22] including Li-rich layered oxides with oxygen redox.[23–29] For $LiCoO_2$, the oxygen redox reaction has been investigated by O K RXES,[30,31] but the reaction occurs at voltage around 4.6 V *vs.* Li/Li^+, which is higher than the voltage range in which the Co^{3+}/Co^{4+} redox occurs in practical applications (below ~4.2 V *vs.* Li/Li^+). Here, we report a Co L_3 (2p–3d–2p resonance) *ex situ* RXES study of $LiCoO_2$ in three states (the initial state, the 4.2-V charged state, and the discharged state after 4.2-V charging) to clarify the intrinsic role of the O 2p–Co 3d CT effect in the redox reaction below 4.2 V.

2. Method

$LiCoO_2$ powder was fabricated by following the procedure below. First, $CoCl_2{\cdot}6H_2O$ (0.0025 mol) and $LiNO_3$ (0.020 mol) were dissolved in H_2O (10 ml). The solution was then dried at 140 °C in vacuum for 17 h. The dried reactant was placed in a Al_2O_3 crucible with a lid. The crucible was placed in a muffle furnace and heated at 800 °C in air for 3 h. Finally, the sample was washed with deionized water and dried under vacuum conditions. The $LiCoO_2$ powder was pasted with super-P Li as a carbon additive to increase the conductivity and polytetrafluoroethylene as a binder. The paste was then pressed onto Al mesh as a current collector to fabricate the working electrode. A three-electrode beaker cell was assembled with the $LiCoO_2$ working electrode, a Li–metal counter electrode, a Li–metal reference electrode, and a 1 M $LiClO_4$/ethylene carbonate–diethyl carbonate electrolyte solution. The charge/discharge experiments of the beaker cells were performed by cyclic voltammetry (CV). The scan speed was set to 0.5 mV s^{-1}, and the cutoff voltages were 4.2 V (*vs.* Li/Li^+) for charging and 3.0 V for discharging. The charged/discharged $LiCoO_2$ samples were removed from the cell in a glove box, and they were then transferred to a vacuum chamber using a transfer vessel without exposure to air.

The XAS measurements were performed at BL07LSU of SPring-8[32] using the surface-sensitive total-electron yield (TEY) mode. The RXES experiments were performed using the ultrahigh-resolution X-ray emission spectrometer HORNET at BL07LSU of SPring-8.[33] The energy resolution of the incident beam was 100 meV, and the total energy resolution for the RXES measurements was ΔE = 330 meV at 785.0 eV. All of the XAS and RXES measurements were performed at room temperature. We also performed spectral analyses using Quanty software programs based on CT multiplet calculation.[34,35] In the calculation, the Co 3d orbitals with the Co 2p core–hole effect and O 2p orbitals in a CoO_6 octahedron were considered. To describe the ligand-to-metal CT, configuration interactions were used as a linear combination of the basis of each electron configuration with the CT effect (d^n, $d^{n+1}\underline{L}$, and $d^{n+2}\underline{L}^2$, where $\underline{L}$ denotes a ligand hole).

3. Results and discussion

The CV curves of $LiCoO_2$ are shown in Fig. 1. The voltage range was set to 3.0–4.2 V (*vs.* Li/Li^+). The open-circuit voltage before cycling was 3.2 V. A broad structure was observed around 4.1 V in the charge process. This indicates the oxidation reaction due to Li extraction from $LiCoO_2$. For the discharge process, the reduction peak was observed at 3.8 V owing to reinsertion of Li.

To investigate the unoccupied Co 3d states and select the incident photon energy (excitation energy) for RXES, TEY XAS measurements were performed. The Co L_3-edge TEY XAS results for $LiCoO_2$ are shown in Fig. 2. According to the XAS line profiles in previous reports,[8,9,14] the initial and discharged states are attributed to the Co^{3+} state, suggesting a reversible redox reaction for the Co 3d state. The small multiplet splitting for the initial and discharged states suggests that the e_g orbital is almost unoccupied in the Co^{3+} (d^6) low-spin (LS) state.[14] The LS Co^{3+} has occupied six t_{2g} orbitals (which should be further split into e_g' and a_{1g} orbitals in the lower symmetry as reported in ref. 14) and all the e_g orbitals are empty.

The main peak position in the 4.2-V charged-state spectrum slightly shifted to the higher energy region and the shoulder structures at 776.8–778.4 and 781.0–782.0 eV were enhanced (indicated by the arrows in Fig. 2). These results are similar to those in previous reports.[8–14] The changes for the 4.2-V charged state indicate the appearance of the Co^{4+} state. The slight shift of the main peak suggests oxidation of Co, which should be accompanied with the slight increase of the structure at 781.0–782.0 eV. The increase of the shoulder structure at 776.8–778.4 eV is attributed to t_{2g} hole (on the a_{1g} orbital in the lower symmetry) created by charge.[14] Moreover, it is expected that approximately half of the Co^{3+} sites remained (*i.e.*, approximately 0.5Li was extracted) at the upper cutoff voltage of 4.2 V,

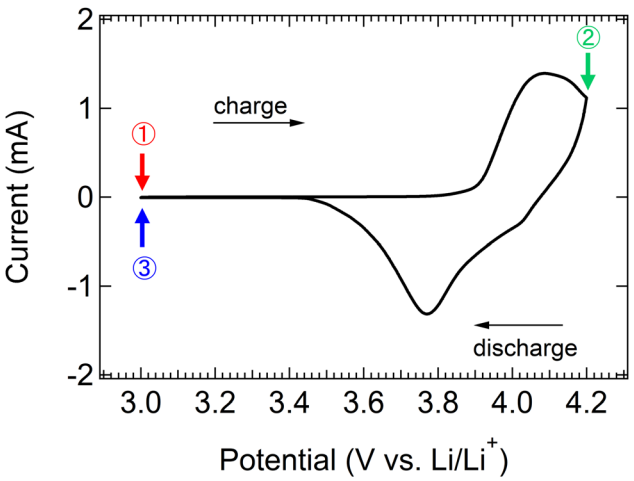

Fig. 1 CV curves of $LiCoO_2$ with a scan speed of 0.5 mV s^{-1}.

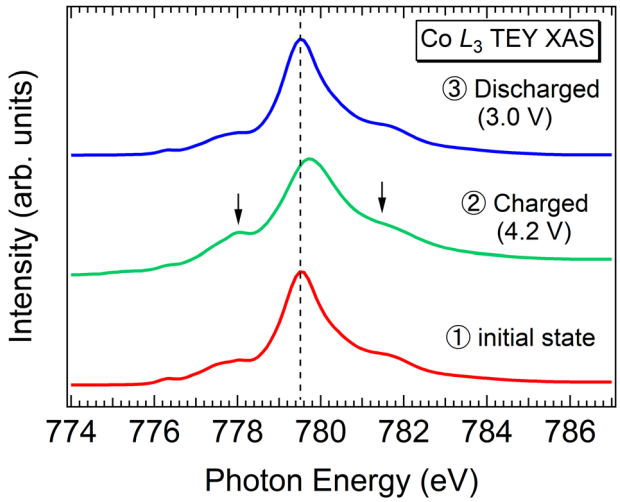

Fig. 2 *Ex situ* Co L_3-edge TEY XAS spectra corresponding to the three states in Fig. 1. The dotted line indicates the excitation energy (779.5 eV) for the RXES measurements.

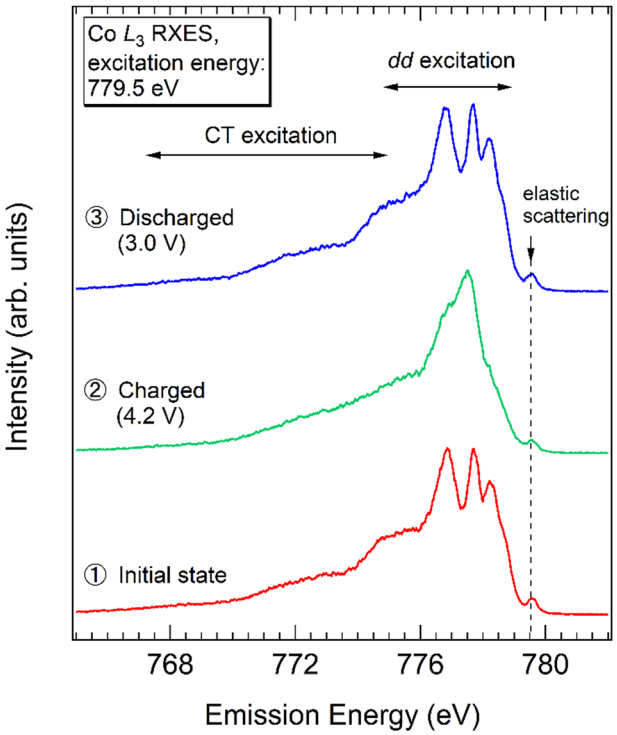

Fig. 3 *Ex situ* RXES results at the Co L_3 edge of $LiCoO_2$ for the three states shown in Fig. 1.

which is usual value for practical use to maintain the host framework.[1,2]

To further investigate the Co^{3+} state in the initial state and determine how it changes by the charge process, the excitation energy for RXES was selected to be 779.5 eV, which is the Co L_3-edge main peak position for the initial and discharged states (indicated by the dashed line in Fig. 2). The same excitation energy was used for the charged sample.

The RXES results at the Co L_3 edge are shown in Fig. 3. The peak at 779.5 eV corresponds to the elastic scattering where the emission energy equals the excitation energy. The sharp peaks from 775.0 to 779.0 eV for the initial state are related to the dd excitations. The broad structure below 775.0 eV is mainly related to the CT excitation between the Co 3d and O 2p orbitals. In addition, some fluorescence components should be involved for the whole range. These features for the initial state are almost the same as those for the discharged state, suggesting a reversible redox reaction of Co, as for the XAS results. The line shape for the 4.2-V charged state is greatly different from those for the initial and discharged states. Large changes in the Co 3d electronic structure by charging were observed for Co L_3 RXES, while Co L_3-edge XAS showed small changes. In particular, the three dd-excitation peaks observed in the initial state greatly changed in the 4.2-V charged state. These changes can be attributed to the partial oxidation of the Co^{3+} state to the Co^{4+} state.

To analyze the RXES spectra, we performed multiplet calculations including CT effects using the Quanty program. The RXES spectrum with 779.5-eV excitation includes a fluorescence component that was not included in the calculation. For the initial state, we also measured the RXES spectrum with 793.8-eV excitation corresponding to the post-edge region of the Co L_3 edge. The RXES spectrum with 793.8-eV excitation (on-resonance for the L_2 edge) below ~780 eV in the emission-energy scale is regarded as the off-resonant spectrum for the L_3 edge. We subtracted the off-resonant spectrum from the on-resonant 779.5-eV RXES spectrum to remove the fluorescence. The subtracted spectrum (spectrum A) is compared with the Co^{3+} CT multiplet calculation with a CoO_6 cluster model in Fig. 4(a). The calculated result well reproduces the experiment, except for slight differences of the peak intensities of the dd excitations around 778 eV. In addition, the elastic scattering at 779.5 eV in the experimental spectrum is not reproduced well, because it depends on the experimental settings, including the polarization of the incident and emitted photons. The electronic-structure parameters used in the calculation are summarized in Table 1. For the calculation, O_h symmetry was considered for simplicity, while it has been reported that the CoO_6 octahedron has trigonal D_{3d} symmetry slightly deforming compared to the O_h symmetry.[36] The crystal-field splitting 10 Dq value of 1.4 eV is sufficiently strong to maintain the d^6 LS state[37,38] considering the Tanabe–Sugano diagram for this configuration. The CT energy (Δ), corresponding to the energy difference of $E(d^7\underline{L}) - E(d^6)$ ($\underline{L}$ is a ligand hole), is 0.6 eV, resulting in a strong CT effect. Indeed, the calculated weight of charge-transferred $d^7\underline{L}$ configuration (52.1%) is higher than that of d^6 configuration (39.0%) as shown in Table 2.

For the 4.2-V charged state, to extract the Co^{4+} component, we performed a difference analysis. Firstly, we subtracted the off-resonant spectrum for the charged state from the on-resonant 779.5-eV RXES spectrum in the same way for the initial state, which is spectrum B in Fig. 4(b). Next, a difference spectrum (spectrum C) was constructed using the formula of [spectrum B (charged)] − 0.5 × [spectrum A (initial)] (Fig. 4(c)). Here, we

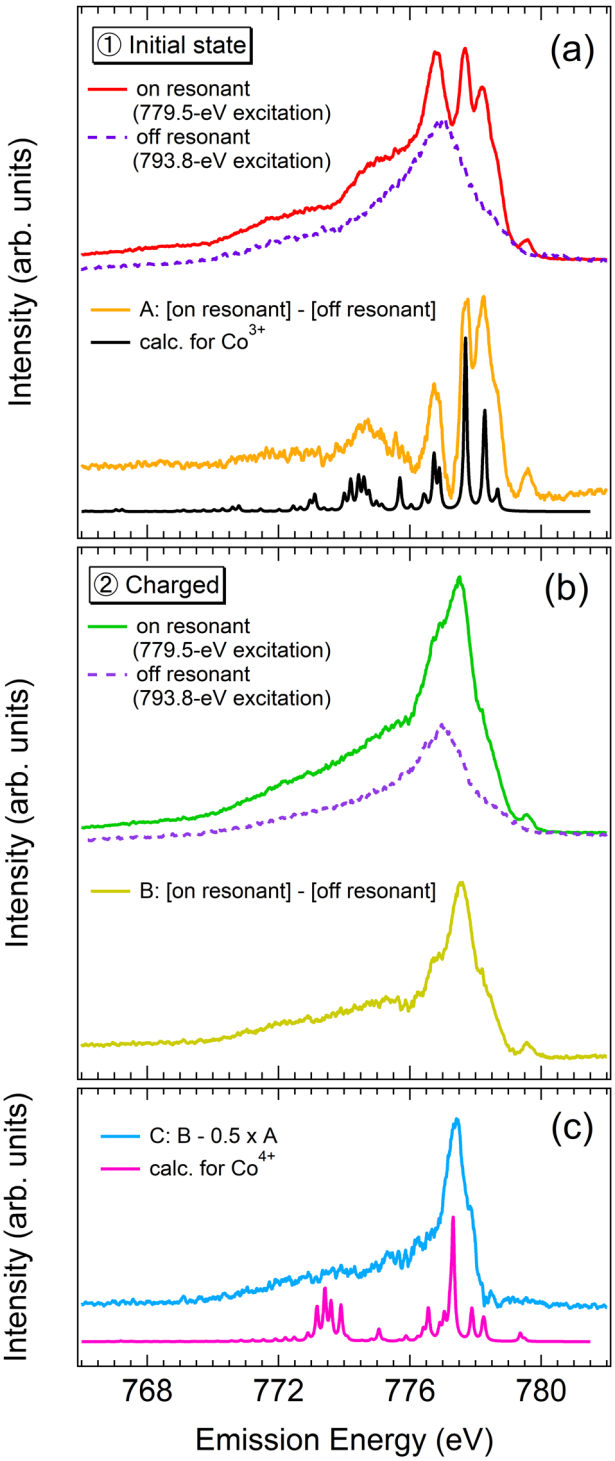

Fig. 4 (a) Subtraction of the off-resonant spectrum from the on resonant spectrum for the initial state and fitting result of the Co^{3+} state. (b) Subtraction of the off-resonant spectrum from the on resonant spectrum for the charged state. (c) Difference analysis for the charged state and fitting result of the Co^{4+} state.

assumed that the Co^{3+} state was unchanged between the initial and charged states. The coefficient of 0.5 in the formula is an assumption based on the nominal chemical equation of $LiCo^{3+}O_2 \Leftrightarrow 0.5Li^+ + 0.5e^- + Li_{0.5}Co^{3.5+}O_2$, while it is difficult to accurately estimate the ratio of Co^{3+}/Co^{4+} from the intensity of RXES spectra.

Table 1 Electronic-structure parameters used in the calculations (in eV)

	Co^{3+} (O_h symmetry)	Co^{4+} (O_h symmetry)
10 Dq	1.4	1.6
Δ	0.6	−1.0
U_{dd}	6.5	7.0
Q	7.5	7.5
$V(e_g)$	2.2	3.0
$V(t_{2g})$	1.1	1.5

Table 2 Calculated weights of each electron configuration and calculated effective 3d electron numbers $\langle n_d \rangle$

Co^{3+} (O_h symmetry)		Co^{4+} (O_h symmetry)	
d^6	39.0%	d^5	27.3%
$d^7\underline{L}$	52.1%	$d^6\underline{L}$	57.1%
$d^8\underline{L}^2$	8.9%	$d^7\underline{L}^2$	15.6%
$\langle n_d \rangle$	6.7	$\langle n_d \rangle$	5.9

The difference in line shape between spectrum C and spectrum A suggests the oxidation reaction of the Co^{3+} LS to Co^{4+} LS states. The shoulder structure of the 777.9-eV peak in the dd excitation region of spectrum C should correspond to the decrease of the 778.3-eV peak in spectrum A, suggesting the removal of an electron from the fully occupied t_{2g} band of the Co^{3+} LS state in the initial state as Fig. 5 shows. Spectrum C was successfully fitted by the Co^{4+} calculation for the dd and CT excitations (Fig. 4(c)). Indeed, the Co^{4+} calculation reproduces the decrease of the 777.9-eV peak. The electronic-structure parameters for the Co^{4+} calculation are summarized in Table 1. For Co^{4+}, Δ is defined as $E(d^6\underline{L}) - E(d^5)$. The Δ value was determined to be −1.0 eV. The negative Δ means that the charge-transferred $d^6\underline{L}$ configuration is considerably dominant compared to the d^5 configuration. Negative Δ in Co^{4+} configuration has been also found for $SrCoO_3$.[39] Indeed, the calculated weight of d^5 configuration is as low as 27.3%, while that of

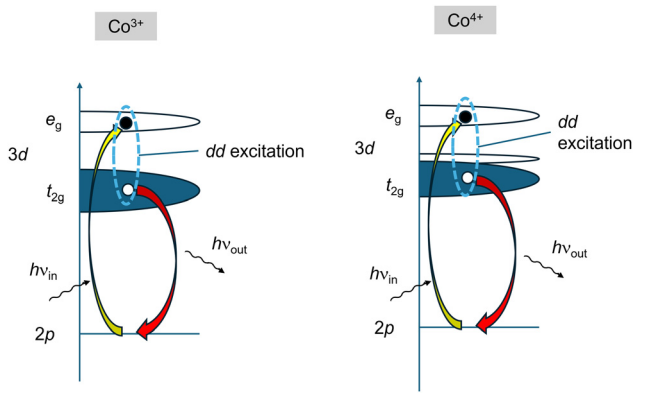

Fig. 5 Schematic images of dd excitation for the Co^{3+} and Co^{4+} states. For simplicity, O_h symmetry is considered. The yellow and red allows indicate the absorption and emission processes. The 779.5-eV excitation of RXES in Fig. 3 and 4 corresponds to the excitation (absorption) to only the e_g band for the Co^{4+} state.

charge-transferred $d^6\underline{L}$ configuration is calculated to be 57.1% (Table 2). The calculated effective 3d electron number $\langle n_d \rangle$ for Co^{4+} is 5.9, which is much larger than 5.0 (Table 2). Moreover, the calculated transfer integral between the Co 3d and O 2p orbitals $V(e_g)$ is 3.0 eV, which suggests that the hybridization of the σ bonding is not weak, and $V(t_{2g})$ for the π bonding is 1.5 eV. Therefore, the CT effect of the Co^{4+} state is further stronger than that of the Co^{3+} state. These results indicate that the O 2p orbital plays an essential role in the redox reaction. The holes created by the charge reaction tend to be located on the p–d hybridized orbital. In that the holes are not localized on the Co 3d orbital, the consideration is partly consistent with previous XAS,[8] X-ray Compton scattering,[7] and theoretical studies[40] which suggest that the hole should be on the O 2p orbital rather than the Co 3d orbital. We conclude that the O 2p–Co 3d hybridized orbital is redox active for $LiCoO_2$.

A similar mechanism has been reported in Mn L-edge XAS and RXES studies of $LiMn_2O_4$ with the Mn^{3+}/Mn^{4+} redox couple[22,41] and Ni L-edge XAS studies of $NaFe_{0.5}Ni_{0.5}O_2$ with the Ni^{3+}/Ni^{4+} redox couple for the Na-ion insertion/extraction.[42] In general, the p–d hybridization in TMOs is particularly important for the physical properties.[43,44] The p–d hybridization in TMOs tends to become stronger for higher oxidation states, such as the tetravalent state.[45] Thus, the redox reaction in TMO-based cathode materials should be considered for the p–d hybridization in the $[TM]O_6$ octahedron rather than the localized 3d orbital of the TM. The situation is different from that for polyanion-type $LiFePO_4$, in which the localized Fe 3d orbital in the FeO_6 octahedron mainly contribute to the redox reaction.[20] $LiFePO_4$ is also a prototypical cathode material, but it should be separately classified from TMO-based cathode materials such as $LiCoO_2$ and $LiMn_2O_4$ in terms of the electronic structure and redox reaction.

The calculated spectra for both the Co^{3+} and Co^{4+} states agreed the experimental RXES spectra (Fig. 4), even though the symmetry in the calculation was simplified to O_h symmetry. One reason for the agreement is that the degree of deformation of the CoO_6 octahedron from O_h symmetry is not large. Another reason is the strong CT effects and strong p–d hybridization. It is most likely that the interaction of the Co–O bond should be very strong, resulting in the symmetry effect not being significant on the RXES spectra. In the near future, we will perform a similar calculation with lower symmetry to further verify the symmetry effect.

4. Conclusions

We have performed *ex situ* RXES at the Co L_3 edge of $LiCoO_2$ in combination with multiplet calculation and succeeded in separately clarifying the valence states of Co^{3+} and Co^{4+}. Both the Co^{3+} and Co^{4+} states show strong CT effects from the O 2p to Co 3d orbitals. The Co^{4+} state in the charged state has a negative CT energy, which means that the charge-transferred $d^6\underline{L}$ configuration is dominant, resulting in an effective 3d-electron number $\langle n_d \rangle$ of 5.9. Similar scenarios have been suggested in previous reports for other typical oxide-based cathode materials like $LiMn_2O_4$. The higher valence state in those oxides, such as the tetravalent state, commonly have strong CT effects. Thus, present and those results indicate that the O 2p orbital plays an essential role in the redox reaction through the strong p–d hybridization in oxide-based cathode materials. In addition, RXES in combination with difference analysis and multiplet calculation is a very powerful method to distinguish a specific oxidation state from mixed valence states. Extracting the higher valence state in the charged state of cathode materials is particularly important to understand the redox reaction. For example, control of the CT effect by some means, such as element substitution based on such electronic-structure analysis using RXES, will be effective to further improve the electrode performance.

Author contributions

D. A., E. H. and A. Y. conceived and directed the project. D. A. and E. H. synthesized and characterized $LiCoO_2$. D. A., H. N., H. M. and E. H. constructed the *operando* cell. T. S., Y. N., R. W. and F. D. G. performed the multiplet calculations. D. A., T. S., H. K., K. Y., J. M., and Y. H. performed the soft X-ray absorption/emission spectroscopy. All of the authors wrote the manuscript.

Data availability

The data that support the findings of this study are available from the corresponding author upon reasonable request.

Conflicts of interest

There are no conflicts to declare.

Acknowledgements

This work was supported by the Ministry of Education, Culture, Sports, Science and Technology (MEXT), Japan; Grant-in-Aid for Specially Promoted Research (No. 15H05701). Part of this work was conducted on the basis of the International Joint Research Program for Innovative Energy Technology by the Ministry of Economy, Trade and Industry (METI), Japan. The XAS and RXES measurements at BL07LSU of SPring-8 were performed by the joint research in SRRO and ISSP, the University of Tokyo (Proposal No. 2017A7531, 2018B7588, 2019B7457, 2020A7477, 2021A7494, 2021A7495, 2021B7429, and 2022A7447).

References

1 K. Mizushima, P. C. Jones, P. J. Wiseman and J. B. Goodenough, *Mat. Res. Bull.*, 1980, **15**, 783–789.
2 K. Mizushima, P. C. Jones, P. J. Wiseman and J. B. Goodenough, *Solid State Ionics*, 1981, **3–4**, 171–174.

3 J. N. Reimers and J. R. Dahn, *J. Elecrochem. Soc.*, 1992, **139**, 2091–2097.
4 J. van Elp, J. L. Wieland, H. Eskes, P. Kuiper, G. A. Sawatzky, F. M. F. de Groot and T. S. Turner, *Phys. Rev. B: Condens. Matter Mater. Phys.*, 1991, **44**, 6090–6103.
5 J. Sugiyama, H. Nozaki, J. H. Brewer, E. J. Ansaldo, G. D. Morris and C. Delmas, *Phys. Rev. B: Condens. Matter Mater. Phys.*, 2005, **72**, 144424.
6 M. Okubo, J. Kim, T. Kudo, H. S. Zhou and I. Honma, *J. Phys. Chem. C*, 2009, **113**, 15337–15342.
7 B. Barbiellini, K. Suzuki, Y. Orikasa, S. Kaprzyk, M. Itou, K. Yamamoto, Y. J. Wang, H. Hafiz, R. Yamada, Y. Uchimoto, A. Bansil, Y. Sakurai and H. Sakurai, *Appl. Phys. Lett.*, 2016, **109**, 073102.
8 Y. Uchimoto, H. Sawada and T. Yao, *J. Synchrotron Radiat.*, 2001, **8**, 872–873.
9 W.-S. Yoon, K.-B. Kim, M.-G. Kim, M.-K. Lee, H.-J. Shin, J.-M. Lee, J.-S. Lee and C.-H. Yo, *J. Phys. Chem. B*, 2002, **106**, 2526–2532.
10 V. R. Galakhov, E. Z. Kurmaev, S. Uhlenbrock, M. Neumann, D. G. Kellerman and V. S. Gorshkov, *Solid State Commun.*, 1996, **99**, 221–224.
11 V. R. Galakhov, M. Neumann and D. G. Kellerman, *Appl. Phys. A: Mater. Sci. Process.*, 2009, **94**, 497–500.
12 V. R. Galakhov, N. A. Ovechkina, A. S. Shkvarin, S. N. Shamin, E. Z. Kurmaev, K. Kuepper, A. F. Takács, M. Raekers, S. Robin, M. Neumann, G.-N. Gavrila, A. S. Semenova, D. G. Kellerman, T. Käämbre and J. Nordgren, *Phys. Rev. B: Condens. Matter Mater. Phys.*, 2006, **74**, 045120.
13 D. Ensling, A. Thissen, S. Laubach, P. C. Schmidt and W. Jaegermann, *Phys. Rev. B: Condens. Matter Mater. Phys.*, 2011, **82**, 195431.
14 T. Mizokawa, Y. Wakisaka, T. Sudayama, C. Iwai, K. Miyoshi, J. Takeuchi, H. Wadati, D. G. Hawthorn, T. Z. Regier and G. A. Sawatzky, *Phys. Rev. Lett.*, 2013, **111**, 056404.
15 C. J. Partridge, C. T. Love, K. E. Swider-Lyons, M. E. Twigg and D. E. Ramaker, *J. Solid State Chem.*, 2013, **203**, 134–144.
16 J. M. Rosolen, P. Ballirano, M. Berrettoni, F. Decker and M. Gregorkiewitz, *Ionics*, 1997, **3**, 345–354.
17 A. Kotani and S. Shin, *Rev. Mod. Phys.*, 2001, **73**, 203–246.
18 L. J. Ament, M. van Veenendaal, T. P. Devereaux, J. P. Hill and J. van den Brink, *Rev. Mod. Phys.*, 2011, **83**, 705–767.
19 F. de Groot and A. Kotani, *Core level spectroscopy of solids*, CRC Press, Boca Raton, Florida, 2008.
20 D. Asakura, Y. Nanba, Y. Makinose, H. Matsuda and E. Hosono, *ChemPhysChem*, 2018, **19**, 988–992.
21 D. Asakura, Y. Nanba, Y. Makinose, H. Matsuda and E. Hosono, *Phys. Chem. Chem. Phys.*, 2017, **19**, 16507–16511.
22 D. Asakura, Y. Nanba, E. Hosono, M. Okubo, H. Niwa, H. Kiuchi, J. Miyawaki and Y. Harada, *Phys. Chem. Chem. Phys.*, 2019, **21**, 18363–18369.
23 T. Sudayama, K. Uehara, T. Mukai, D. Asakura, X.-M. Shi, A. Tsuchimoto, B. Mortemard de Boisse, T. Shimada, E. Watanabe, Y. Harada, M. Nakayama, M. Okubo and A. Yamada, *Energy Environ. Sci.*, 2020, **13**, 1492–1500.
24 W. E. Gent, K. Lim, Y. F. Liang, Q. H. Li, T. Barnes, S. J. Ahn, K. H. Stone, M. Mclntire, J. Y. Hong, J. H. Song, Y. Y. Li, A. Mehta, S. Ermon, T. Tyliszczak, D. Kilcoyne, D. Vine, J. H. Park, S. K. Doo, M. F. Toney, W. L. Yang, D. Prendergast and W. C. Chueh, *Nat. Commun.*, 2017, **8**, 2091.
25 K. Luo, M. R. Roberts, R. Hao, N. Guerrini, D. M. Pickup, Y.-S. Liu, K. Edström, J.-H. Guo, A. V. Chadwick, L. C. Duda and P. G. Bruce, *Nat. Chem.*, 2016, **8**, 684–691.
26 R. A. House, U. Maitra, M. A. Pérez-Osorio, J. G. Lozano, L. Jin, J. W. Somerville, L. C. Duda, A. Nag, A. Walters, K.-J. Zhou, M. R. Roberts and P. G. Bruce, *Nature*, 2020, **577**, 502–508.
27 R. A. House, G. J. Rees, M. A. Pérez-Osorio, J. G. Lozano, J.-J. Marie, E. Boivin, A. W. Robertson, A. Nag, M. Garcia-Fernandez, K.-J. Zhou and P. G. Bruce, *Nat. Energy*, 2020, **5**, 777–785.
28 R. A. House, J.-J. Marie, M. A. Pérez-Osorio, G. J. Rees, E. Boivin and P. G. Bruce, *Nat. Energy*, 2021, **6**, 781–789.
29 L. Massel, K. Hikima, H. Rensmo, K. Suzuki, M. Hirayama, C. Xu, R. Younesi, Y.-S. Liu, J.-H. Guo, R. Kanno, M. Hahlin and L.-C. Duda, *J. Phys. Chem. C*, 2019, **123**, 28519–28526.
30 J.-N. Zhang, Q. Li, C. Ouyang, X. Yu, M. Ge, X. Huang, E. Hu, C. Ma, S. Li, R. Xiao, W. Yang, Y. Chu, Y. Liu, H. Yu, X.-Q. Yang, X. Huang, L. Chen and H. Li, *Nat. Energy*, 2019, **4**, 594–603.
31 E. Hu, Q. Li, X. Wang, F. Meng, J. Liu, J.-N. Zhang, K. Page, W. Xu, L. Gu, R. Xiao, X. Huang, L. Chen, W. Yang, X. Yu and X.-Q. Yang, *Joule*, 2021, **5**, 720–736.
32 S. Yamamoto, Y. Senba, T. Tanaka, H. Ohashi, T. Hirono, H. Kimura, M. Fujisawa, J. Miyawaki, A. Harasawa, T. Seike, S. Takahashi, N. Nariyama, T. Matsushita, M. Takeuchi, T. Ohata, Y. Furukawa, K. Takeshita, S. Goto, Y. Harada, S. Shin, H. Kitamura, A. Kakizaki, M. Oshima and I. Mastuda, *J. Synchrotron Radiat.*, 2014, **21**, 352–365.
33 Y. Harada, M. Kobayashi, H. Niwa, Y. Senba, H. Ohashi, T. Tokushima, Y. Horikawa, S. Shin and M. Oshima, *Rev. Sci. Instrum.*, 2012, **83**, 013116.
34 M. W. Haverkort, M. Zwierzcki and O. K. Andersen, *Phys. Rev. B: Condens. Matter Mater. Phys.*, 2012, **85**, 165113.
35 R.-P. Wang, B. Liu, R. J. Green, M. U. Delgado-Jaime, M. Ghiasi, T. Schmitt, M. M. van Schooneveld and F. M. F. de Groot, *J. Phys. Chem. C*, 2017, **121**, 24919–24928.
36 H.-J. Kim, Y. U. Jeong, J.-H. Lee and J.-J. Kim, *J. Power Sources*, 2006, **159**, 233–236.
37 D. Qian, Y. Hinuma, H. Chen, L.-S. Du, K. J. Carroll, G. Ceder, C. P. Grey and Y. S. Meng, *J. Am. Chem. Soc.*, 2012, **134**, 6096–6099.
38 L. A. Montoro, M. Abbate and J. M. Rosolen, *Electrochem. Solid State Lett.*, 2000, **3**, 410–412.
39 R. H. Potze, G. A. Sawatzky and M. Abbate, *Phys. Rev. B: Condens. Matter Mater. Phys.*, 1995, **51**, 11501–11506.
40 Y. Yamauchi and H. Nakai, *J. Electrochem. Soc.*, 2013, **160**, A1364–A1368.
41 D. Asakura, E. Hosono, H. Niwa, H. Kiuchi, J. Miyawaki, Y. Nanba, M. Okubo, H. Matsuda, H. S. Zhou, M. Oshima and Y. Harada, *Electrochem. Commun.*, 2015, **50**, 93–96.
42 Y. Nanba, T. Iwao, B. Mortemard de Boisse, W. Zao, E. Hosono, D. Asakura, H. Niwa, H. Kiuchi, J. Miyawaki,

Y. Harada, M. Okubo and A. Yamada, *Chem. Mater.*, 2016, **28**, 1058–1065.
43 M. Imada, A. Fujimori and Y. Tokura, *Rev. Mod. Phys.*, 1998, **70**, 1039–1263.
44 A. Fujimori and F. Minami, *Phys. Rev. B: Condens. Matter Mater. Phys.*, 1984, **30**, 957–971.
45 K. Kawai, D. Asakura, S.-I. Nishimura and A. Yamada, *Chem. Commun.*, 2019, **55**, 13717–13720.